SYNTHESIS, CHARACTERIZATION, DNA INTERACTIONS, FGF GROWTH RECEPTOR INTERACTION AND BIOLOGICAL SCREENING OF SCHIFF BASE METAL(II) COMPLEXES INCORPORATING BENZIMIDAZOLE AND TERPYRIDINE NNO DONOR LIGANDS

GANESAN KUMARAVEL

Department of Chemistry, Nadar Mahajana Sangam S.Vellaichamy Nadar College (Autonomous), Madurai-625 019, Tamil Nadu, India

chemistrykumaravel@gmail.com

ABSTRACT

In the quest for novel treatment against safe life form, the alteration of existing medication by mix to a metal focus has picked up consideration as of late. Thus, metal-based drug is seen as promising alternatives for possible replacement for some of the current drugs. So, we synthesized Schiff base metal complexes in this regard. The present paper deals with the synthesis and characterization of metal complexes of tridentate Schiff base ligand derived from the inserted condensation of 8-aminoquinoline with p-nitrosalicylaldehyde in a 1:1 molar ratio. Using this tridentate ligand, complexes with general formula ML_2 has been synthesized. The synthesized complex was characterized by several techniques using molar conductance, elemental analysis, FT-IR, electronic absorption, EPR, mass and NMR spectroscopy. The elemental analysis data suggest the stoichiometry to be 1:2 [M:L]. The complex is non-electrolytic in nature as suggested by molar conductance measurements. Infrared spectral data indicate the coordination between the ligand and the central metal ion through deprotonated phenolic oxygen, nitrogen of quinoline ring and azomethine nitrogen atom. Spectral studies suggest octahedral geometry for the complexes. The anticancer activity of Schiff base ligand and its metal complexes was also studied against breast and colon cell lines. The metal complexes showed IC_{50} higher than that of L, especially the Cu(II) complex which showed the highest IC_{50} against breast cell line.

Keywords: Molecular docking; Schiff base metal complexes; DNA binding studies; gel electrophoresis; cytotoxicity.

INTRODUCTION

Almost every second person diagnosed with cancer dies due to noneffective therapy [1]. Chemotherapy, surgery and radiotherapy are general directions in cancer treatment. For many years, laboratories all over the world have been conducting research on new and more effective drugs that show fewer side effects. Despite substantial progress in the field, no compound has been developed that satisfies the expectations of both, patients and doctors. This problem relates to the resistance of many types of cancer to drugs, to undesirable side effects caused by currently prescribed drugs, to their low specificity, or to the necessity of using many

different cytostatic drugs in long-term combination treatment [2]. Therefore, the search of new compounds with anticancer activity is one of the fundamental tasks of medicinal chemistry [3].

The chemistry of metal complexes among Schiff base ligands and their applications has fascinated considerable attention, mainly due to their preparative accessibility, structural variability, magnetic properties and biological properties [4-8]. Metal complexes of Schiff base have played a central role in the development of coordination chemistry [9]. Various Schiff base complexes have been far and wide studied because they have antimicrobial, anticancer, anti-inflammatory, analgesic, antifertility, and herbicidal applications [10, 11]. Chelating ligands containing N, N, and O donor atoms show broad biological activity and are of special interest because of the ways in which they are bonded to the metal ions [12]. It is known that existence of metal ions bonded to biologically active compounds may enhance their activities [13–15]. Recently, there has been considerable interest in NNN, NNO, ONO donor type tridentate Schiff base ligands. In such species all three donor sites can coordinate to a metal ion [4-7]. Interestingly, in these type complexes, the coordination vacancies of metal ion are saturated by solvent and/or bridging ligand which represents pseudohalide groups, N^{3-}, SCN^{-}, OCN^{-}, having a tendency to bond mononuclear complex groups via μ-bridges to form polynuclear complexes [4, 5]. Also, pseudohalogens complexes with transition metal have attracted much interest due to their structures, magnetic properties and their versatile behaviors as bridging ligands in end-to-end and/or end-on fashions [6]. Although many coordination compounds of tridentate Schiff base have been studied, the researchers have been rarely reported structures of the $[ML_2]$, (M=Cu, Co, Ni, Zn; L=NNO donor atoms) type [7, 8, 16].

Many antitumor drugs are designed to target DNA because the interaction between drugs and DNA can cause DNA damage and show toxic and antitumor effects [17-21]. Significant side effects of cisplatin have limited the clinical applications and motivated extensive investigations into alternative metal-based cancer therapies. The quinoline skeleton is present in numerous natural products, especially in alkaloids. Many quinolines display interesting pharmacological activities and have found applications as pharmaceuticals, *e.g.*, antimalarial drugs, such as quinine or chloroquin. Hydroxyquinolines derivatives were reported to be promising therapeutic agents for Alzheimer's dementia due to strong complexation with copper and zinc ions which are involved in the ß-amyloid peptide aggregation that causes neuronal loss in Alzheimer's disease patients [22-25]. Moreover, hydroxyquinolines are known to exhibit a variety of biological activities [26-30]. In particular, clioquinol (5-chloro-7-iodo-quinolin-8-ol) is currently commercially available as an antifungal and antibacterial drug.

Regarding the anticancer activity of the hydroxyquinolines, a number of interesting features were highlighted. They are classified as proteasome inhibitors through complexation with copper ions [31-34]; they induce apoptosis of human cancer cell lines by targeting zinc to lysosomes [35]; they are NF-kappa inhibitors [36,37], or stimulate macrophages to release tumor necrosis factor alpha [38] among other anticancer activities. All these applications are related to the use of hydroxyquinolines as scavengers of metals involved in the pathogenesis of various diseases. Even though many Schiff bases using salicylaldehyde and substituted salicylaldehydes and amines had been studied [39-42] as ligands, no work had been done with *p*-nitrosalicylaldehyde and 8-aminoquinoline as the basic nucleus of Schiff bases. Schiff base metal complexes had been a broadly studied subject to their industrial and biological

applications. Recently, we have synthesized new Cu, Co, Ni and Zn complexes containing hydroxyquinolines in their structure and could demonstrate high *in vitro* antitumor activity and their interactions with DNA.

Experimental

Reagents and instruments

The chemicals involved in this work were of AnalaR grade and were used without further purification. However, the solvents were purified by following the standard procedures [43]. 8-aminoquinoline, *p*-nitrosalicylaldehyde, CT-DNA, pBR322 DNA and ethidium bromide were obtained from Sigma-Aldrich. Solvents ethanol, dimethylformamide and agar were procured from Hi-media chemicals. All the metal salts were received from E-Merck. DNA was purchased from Bangalore Genei (India).

Physical methods such as IR, UV-Vis., NMR, EPR, ESI-MS, electrochemical measurements, magnetic susceptibility, molar conductance, DNA binding, cleavage, antimicrobial and cytotoxic activity were followed according to the previously reported procedures [44, 45].

Synthesis of Schiff base Ligand (L)

The synthesis of Schiff base ligand (**L)** was prepared by the condensation of 8-aminoquinoline (5mmol) dissolved in 15 mL of ethanol solution and then condensed with the solution *p*-nitrosalicylaldehyde (5mmol) in ethanol (10 mL). The condensed mixture was then refluxed for 3 h and the yellow solid precipitated on cooling. It was filtered and washed with hot ethanol first, then pet-ether and dried. Further, it was recrystallized in a hot solution of ethanol–methanol (1:1) and dried *in vacuo*.

[L], Yield: 74 %. Anal. Calc. for $C_{16}H_{11}N_3O_3$: C, 65.5; H, 3.8; N, 14.3 %; Found C, 65.1; H, 3.6; N, 14.0 %. IR data (KBr, cm^{-1}): 1648 ν(CH=N), 1245 ν(C-O), 3418 ν(OH). ^{1}H NMR (DMSO-d_6) ppm: 7.49-8.83; 7.77-7.92 (aromatic: 8-AQ; *p*-NS) (m), 8.87 (CH=N) (s), 5.35 (OH) (s). ^{13}CNMR (ppm): 121.5–153.9 (C_1 to C_9), 160.0 (C_{10}), 111.6–162.0 (C_{11} to C_{16}). λ_{max} (DMF, cm^{-1}): 36,764, 30,581.

Synthesis of metal(II) complexes

The procedure for synthesizing the metal complexes of the type $[ML_2]$ is as follows: the synthesized ligand **L** (10 mmol) was dissolved in a hot ethanolic solution and refluxed with the appropriate metal(II) chloride salts [Cu(II), Co(II), Ni(II) and Zn(II)] (5 mmol) on a rotamantle for 2 h. On cooling the product obtained was washed with hot ethanol, pet-ether and then dried. Further, it was recrystallized in a hot solution of ethanol–methanol (1:1) and dried *in vacuo*.

$[CuL_2]$ (1) Yield: 72 %. Anal. Calc. For $C_{32}H_{20}Cu\ N_6O_6$, C, 59.3; H, 3.1; N, 13.0; Cu, 9.8 %. Found: C, 58.7; H, 2.9; N, 12.7; Cu, 9.5 %. IR (KBr pellet, cm^{-1}): 1619 ν(CH=N), 1227 ν(C-O), 536 (M-O) and 432 (M-N). $\Lambda_M\ 10^{-3}$ ($ohm^{-1}\ cm^2\ mol^{-1}$) =19.5. λ_{max} (DMF, cm^{-1}): 36,231, 31,446, 13,793. μ_{eff} (BM): 1.85.

[CoL$_2$] (2) Yield: 68 %. Anal. Calc. for $C_{32}H_{20}CoN_6O_6$, C, 59.7; H, 3.1; N, 13.1; Co, 9.2 %. Found: C, 59.4; H, 3.0; N, 12.8; Co, 8.8 %. IR (KBr pellet, cm^{-1}): 1604 ν(CH=N), 1234 ν(C-O), 521 (M-O) and 438 (M-N). Λ_M 10^{-3} (ohm^{-1} cm^2 mol^{-1}) =13.7. λ_{max} (DMF, cm^{-1}): 13,368, 16,233, 24,390. μ_{eff} (BM): 4.76.

[NiL$_2$] (3) Yield: 70 %. Anal. Calc. for $C_{32}H_{20}NiN_6O_6$, C, 59.8; H, 3.1; N, 13.1; Ni, 9.1 %. Found: C, 59.2; H, 3.0; N, 12.6; Ni, 8.7 %. IR (KBr pellet, cm^{-1}): 1626 ν(CH=N), 1223 ν(C-O), 527 (M-O) and 421 (M-N). Λ_M 10^{-3} (ohm^{-1} cm^2 mol^{-1}) =15.1. λ_{max} (DMF, cm^{-1}): 14,005, 18,018, 20,790. μ_{eff} (BM): 3.18.

[ZnL$_2$] (4) Yield: 69 %. Anal. Calc. for $C_{32}H_{20}ZnN_6O_6$, C, 59.1; H, 3.1; N, 12.9; Zn, 10.1 %. Found: C, 58.5; H, 2.9; N, 12.4; Zn, 9.7 %. IR (KBr pellet, cm^{-1}): 1608 ν(CH=N), 1231 ν(C-O), 515 (M-O) and 416 (M-N). ^{1}H NMR (DMSO-d_6) ppm: 7.49-8.83; 7.77-7.92 (aromatic: 8-AQ; *p*-NS) (m), 9.43 (CH=N) (s). ^{13}CNMR (ppm): 125.4–146.7 (C_1 to C_9), 157.4 (C_{10}), 111.5–158.5 (C_{11} to C_{16}). Λ_M 10^{-3} (ohm^{-1} cm^2 mol^{-1}) = 18.3. λ_{max} (DMF, cm^{-1}): 32,051, 29,411. μ_{eff} (BM): diamagnetic.

RESULTS AND DISCUSSION

Elemental analysis and molar conductance

The synthesized complexes are analyzed for the presence of elements using CHN analyzer. The obtained results of elemental analysis for all the complexes are in good agreement with the calculated values. According to the data, the complexes are in 2:1 ratio [Ligand: Metal]. Thus the metal complexes can be categorized under the type [ML$_2$] wherein the L acts as tridentate donor. The electrolytic nature of the mononuclear metal complexes was deduced from their molar conductivities which were measured in DMF at 10^{-3} M. The values of all the complexes have been found in the range 13.7-19.5 ohm^{-1} cm^2 mol^{-1} indicating their non-electrolytic nature according to Geary [46]. The absence of counter ion (chloride) was confirmed by the Volhard's test.

Infrared spectra

IR spectrum of the free Schiff base was compared with those of the complexes in order to infer the coordination mode. In the spectrum of the ligand, a sharp peak at 1648 cm^{-1} is due to the azomethine (–CH=N–) group. The strong band observed at 1648 cm^{-1} is shifted to lower wave number by 44–22 cm^{-1} in the spectra of metal(II) complexes. The lowering of wave number may be attributed to the decrease in electron density on the nitrogen atom of the azomethine group [47]. This indicates the coordination of azomethine (–CH=N–) group to the metal ion in complexes. The presence of band observed at 3418 cm^{-1} is attributed to ν(OH) stretching frequencies of *p*-nitrosalicylaldehyde moiety. The absence of these bands in the complexes indicates the coordination of ν(OH) group through deprotonation [58]. This is further evidenced by the ν(C-O) band in these complexes (1234–1223 cm^{-1}), appearing at lower frequencies compared to that of the ligand (1245 cm^{-1}) [49]. Further, the non-ligand bands in the region 515–536 cm^{-1} and 416–438 cm^{-1} are due to the formation of M–O and M–N bonds respectively [50]. In conclusion, these data suggest an ONN tridentate behavior of the ligand.

Electronic spectra and magnetic moments

Electronic spectra of the ligand and its complexes were measured in DMF. The free ligand exhibited strong band at 36,764 cm^{-1} due to intra-ligand $\pi \rightarrow \pi^*$ transitions, these bands remain almost unchanged in the spectra of complexes. Absorption in the band at 30,581 cm^{-1} is attributed to the $n \rightarrow \pi^*$ transition associated with azomethine, the bathochromic shift of this absorption upon complexation is due to the donation of a lone pair of electrons to the metal ion, indicating the coordination of azomethine nitrogen [51,52]. $[CoL_2]$ complex possesses a magnetic moment of 4.76 BM, which is in agreement with values reported for three unpaired electrons in an octahedral environment. The lowest energy band at 13,368 cm^{-1} was due to $^4T_{1g} \rightarrow {}^4T_{2g}$ (ν_1) and broad band's near 16,233 and 24,390 cm^{-1} were assigned to $^4T_{1g} \rightarrow {}^4A_{2g}$ (ν_2) and $^4T_{1g} \rightarrow {}^4T_{1g}$ (P) (ν_3) transitions respectively, supporting an octahedral geometry for the complex [54]. However, $[NiL_2]$ exhibits a magnetic moment of 3.18 BM, consistent with octahedral geometry [53]. The electronic spectrum of $[NiL_2]$ displayed d–d transitions around 14,005, 18,018 and 20,790 cm^{-1}, assignable to $^3A_{2g} \rightarrow {}^3T_{2g}$ (ν_1), $^3A_{2g} \rightarrow {}^3T_{1g}$ (ν_2) and $^3A_{2g} \rightarrow {}^3T_{1g}$ (P) (ν_3) transitions respectively, indicating an octahedral geometry. The $[CuL_2]$ complex in the present study shows a μ_{eff} value of 1.85 B.M, corresponding to one unpaired electron [54]. The absorption spectrum of this complex exhibits broad d–d electronic band centered at 13,793 cm^{-1}, assignable to $^2E_g \rightarrow {}^2T_{2g}$ transition [55]. Absorptions in this region are typical of species with octahedral geometry around the Cu(II) ions. Finally, the $[ZnL_2]$ complex shows bands at 32,051 and 29,411 cm^{-1}, which are due to the intra ligand transitions [56]. The empirical formulae of the complex suggest that the Zn(II) complex also exhibit octahedral geometry.

Nuclear magnetic resonance spectra

The clearest characterization of the synthesized compounds can be seen from the ^1H NMR and ^{13}C NMR spectrums in DMSO-d_6. ^1H NMR spectrum of ligand shows multiplet at 7.49-8.83 ppm (8-AQ) and 7.77-7.92 ppm (*p*-NS) due to the presence of aromatic protons [57]. There is a singlet at 8.87 ppm characteristic of azomethine proton, an additional peak at 5.35 ppm belonging to the –OH proton present in the *p*-nitrosalicylaldehyde ring is also observed. In the ^1H NMR spectrum of the Zn(II) complex, the azomethine proton signal is shifted downfield to 9.43 ppm as compared to the free ligand due to the deshielding of the azomethine group owing to the coordination with Zn(II) ion [58]. It is clearly an indication of azomethine nitrogen involvement in coordination with Zn(II). In comparison with ^1H NMR spectrum of **L**, there is no noticeable change in the aromatic proton signals of $[ZnL_2]$.

The ^{13}C NMR spectrum of **L** exhibits aromatic carbon signals in the range 121.5–153.9 ppm (8-AQ) and 111.6–162.0 ppm (*p*-NS). It also exhibits another important peak at 160.0 ppm, characteristic of -HC=N bond. In the case of $[ZnL_2]$, such distinctive peak of -HC=N bond gets shifted to 157.4 ppm. The ligand also shows a peak for –C-OH at 162.0 ppm which is shifted towards downfield at 158.5 ppm indicating the coordination of –C-O with Zn(II) ion. This evidence of C-O group greatly supports the coordination of oxygen with Zn(II) metal centre. The oxygen atom coordinated with central metal atom is further supported by infrared spectra.

Mass spectra

The mass spectra and the molecular ion peaks confirmed the proposed formulae of the complexes. Generally, the fragmentation patterns of the complexes showed similar fragments

to those of the Schiff base ligand. The ESI mass spectrum of ligand showed a molecular ion peak at m/z = 231.2 amu corresponding to [M + H]+, which confirms the proposed formula. It also shows a series of peaks at 233.2, 214, 186, and 130 corresponding to various fragments. The intensities of these peaks give the idea of the stability of the fragments. ESI mass spectrum of the metal(II) complexes showing the fragmentation model beside the m/z peak value are

Finally, from the interpretation of elemental and spectral data (infrared, electronic, mass and EPR) as well as magnetic susceptibility measurements at room temperature and conductivity measurements, it is possible to draw up the tentative structures of the metal complexes. Scheme 1 represents the proposed structures of the metal complexes.

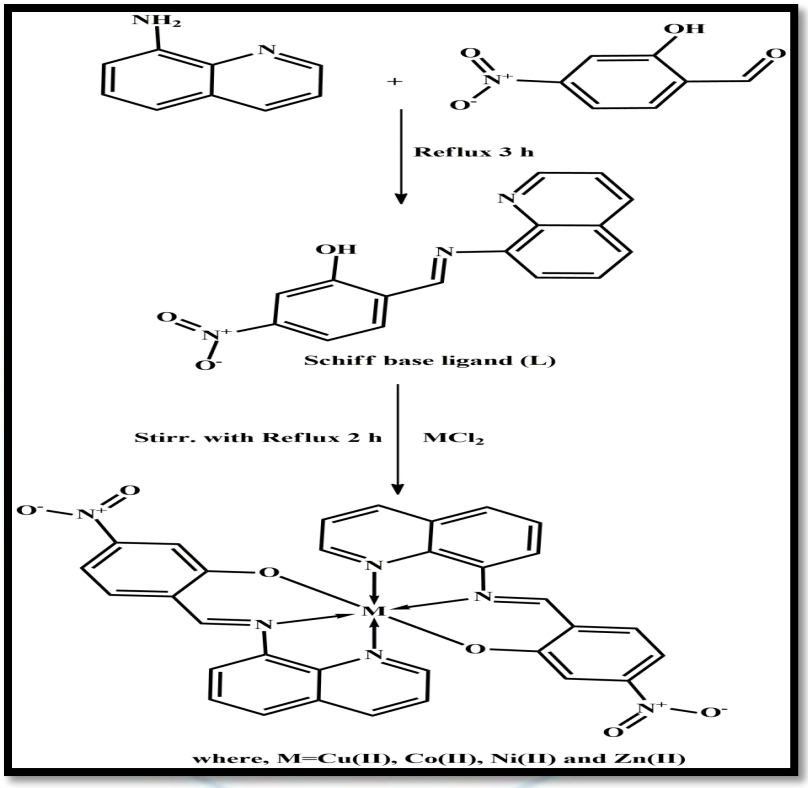

Scheme 1. Synthesis of Schiff base ligand (L) and its metal(II) complexes.

DNA binding studies

Absorption spectral titrations

It is generally accepted that DNA is the primary pharmacological target of many metal based antitumor agents. The binding activities of DNA–metal complexes have been a clue of paramount importance for understanding the mechanism of effective metal based chemotherapeutic drugs [59]. Herein, the interaction between complexes and CT-DNA was characterized by UV–Vis absorption spectroscopy. The absorption spectrum of copper complex in the absence and presence of CT-DNA at different concentrations are given in Fig. 1. Upon increasing the concentration of CT-DNA to the test compounds, the absorption band of the ligand exhibited hypochromism of 10.8 % with red shift of 2 nm at 298 nm, whereas the absorption bands of complexes **1-4** exhibited a hypochromism of about 30.4 % at 341 nm, 22.1 % at 328 nm, 19.0 % at 324 nm and 18.1 % at 314 nm with red shifts of

2-3 nm, respectively. These results suggested an intimate association of the test compounds with CT-DNA, and it is also likely that these compounds bind to the DNA helix via intercalation. After the compounds intercalate to the base pairs of DNA, the π orbital of the intercalated compounds could couple with π orbitals of the base pairs, thus decreasing the π to π* transition energies, hence resulting in hypochromism [60]. In order to compare quantitatively the binding strength of the compounds, the intrinsic binding constants (K_b) of them with CT-DNA were determined from the following equation [61].

$$DNA]/(\varepsilon_a–\varepsilon_f) = [DNA]/(\varepsilon_b–\varepsilon_f) + [K_b(\varepsilon_b–\varepsilon_f)]^{-1}$$

where [DNA] is the concentration of DNA in base pairs and the apparent absorption coefficient ε_a, ε_f and ε_b correspond to A_{obs}/[complex], the extinction coefficient for the free complex, and the extinction coefficient for the complexes in the fully bound form, respectively. The plot of [DNA]/(ε_a-ε_f) versus [DNA] gave a slope and the intercept which are equal to 1/(ε_b-ε_f) and 1/K_b (ε_b-ε_f), respectively; K_b is the ratio of the slope to the intercept. The magnitudes of intrinsic binding constants (K_b) were calculated to be 3.4 x 10^5 M^{-1}, 2.8 x 10^5 M^{-1}, 2.4 x 10^5 M^{-1} and 2.0 x 10^5 M^{-1} for complexes **1-4** respectively. The observed values of K_b revealed that the metal(II) complexes (**1-4**) bind strongly than the respective ligand to DNA via intercalative binding mode. From the results obtained, it has been found that complex **1** strongly binds with CT-DNA in comparison to that with **2**, **3** and **4**, and binding affinity was in the order **1 > 2 > 3 > 4 > L**. According to the electronic absorption spectrum, we can deduce initially that the complexes can bind to DNA by intercalation, but the binding mode need to be proved through more experiments.

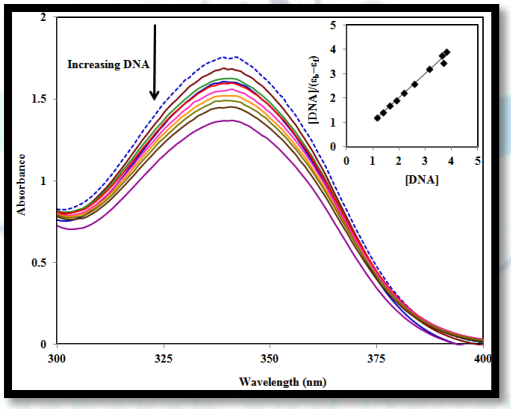

Fig. 1. Electronic absorption spectrum of complex (**1**) in buffer pH = 7.2 at 25 ^{0}C the absence (-----) and presence (—) of increasing amount of CT-DNA.

DNA binding study with viscosity measurements

Spectroscopic data are necessary, but not sufficient to support a binding mode. To further clarify the nature of the interaction between the complex and DNA. Hydrodynamic methods such as viscosity measurements, which are sensitive to length increase or decrease of DNA, are regarded as the most effective means of studying the binding mode of complexes to DNA [62]. The relative viscosity of DNA solution increases significantly as the amount of the complex increases, but the increase is less than that observed for the typical intercalator EB which is consistent with the above absorption spectroscopic result, indicating that intercalative as shown in Fig. 2. This may be due to the insertion of aromatic ring in Schiff base ligand into the DNA base pairs and resulting in a bend in the DNA helix, hence, increase in separation of

the base pairs at the intercalation site, consequently increasing in DNA molecular length. Moreover, the sequence of the observed increase in values of viscosity was correlated the binding affinity to DNA *i.e.* copper complex show the highest binding affinity to DNA and the highest viscosity. The information obtained from this work could be helpful to the understanding of the mechanism of the interaction of small molecules with nucleic acids, and should be useful in the development of potential probes of DNA structure and conformation [63].

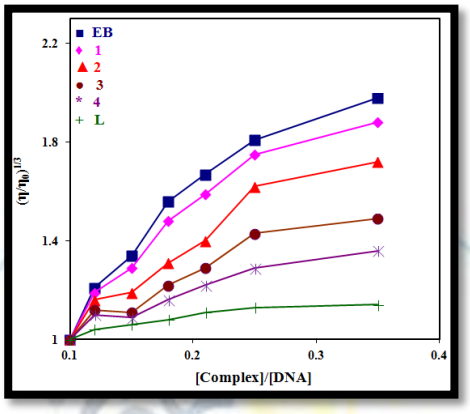

Fig. 2. Effect of increasing amount of [EB] (■), [CuL_2](**1**) (♦), [CoL_2](**2**) (▲),[NiL_2](**3**) (●), [ZnL_2](**4**) (*) and Ligand(**L**) (+) on the viscosity of DNA. R = [complex]/[DNA] or [EB]/[DNA].

DNA interaction using electrochemical studies

Electrochemical techniques are complementary to other related biophysical techniques that are applied to study the interaction between the redox active molecules and biomolecules [64]. The cyclic voltammetric behavior of all the complexes has been examined in the absence and presence of DNA in 5 mM Tris–HCl/50 mM NaCl buffer solution as the supporting electrolyte. No new redox peaks appeared after the addition of CT-DNA to each complex, but the current intensity of all the peaks decreased significantly, suggesting the existence of an interaction between each complex and CT-DNA. Moreover, during DNA addition the anodic peak potential (E_{pa}) shows a positive shift, which is regarded as the proof for the intercalation of the complex into the DNA, because this type of interaction is due to hydrophobic interaction. The cyclic voltammograms of all the studied complexes exhibit peak current ratio approximately unity, which is attributed to the quasi-reversible one electron redox process. All the values corresponding to E_{pc} (V), E_{pa} (V), $E_{1/2}$ (V), ΔE_P and I_{pa}/I_{pc} are listed in Table 1. A significant reduction in their respective peak potentials and cathodic and anodic peak currents can be attributed to a slow diffusion of the equilibrium mixtures of these complexes (free and DNA bound) at the electrode surface. The $E_{1/2}$ shift of these complexes towards positive potential confirms their binding to CT-DNA. However, the positive shift in the E_{pc} or E_{pa} value is indicative of the intercalation of the complex into the DNA double helix while a negative shift reveals the involvement of electrostatic interactions. [65].

The cyclic voltammogram of the [CuL_2] in the absence of CT-DNA featured two anodic peaks. The oxidation of peak E_{Pa1} belongs to Cu(0)/Cu(I) and reduction of Cu(I) occurred, the separation of the anodic and cathodic peak potential is 0.562 V, the ratio of anodic to cathodic

peak currents, ip_a/ip_c=1.12, indicating a quasi-reversible redox process. The oxidation of peak E_{Pa2} belongs to Cu(I)/Cu(II) and reduction of Cu(II) occurred, the separation of the anodic and cathodic peak potential is 0.426 V, the ratio of anodic to cathodic peak currents, ip_a/ip_c=1.38, indicating a quasi-reversible redox process. When CT-DNA is added to a solution of complex both the anodic and cathodic peak current heights of the complex decreased in the same manner of increasing additions of DNA. Also during DNA addition, the anodic peak potential (E_{pa}), cathodic peak potential (E_{pc}), and $E_{1/2}$ (calculated as the average of E_{pc} and E_{pa}) all showed positive shifts. These positive shifts are considered as evidence for intercalation of the complex into the DNA, because this kind of interaction is due to hydrophobic interaction. From the other point of view, if a molecule binds electrostatically to the negatively charged deoxyribose-phosphate backbone of DNA, negative peak potential shifts should be detected. Therefore, the positive shift in the CV peak potentials of complex is indicative of intercalative binding mode of the complex with DNA [66]. The cyclic voltammogram of the [NiL_2] in the absence of CT-DNA featured anodic peak and cathodic peak belong to Ni(I)/Ni(II) and reduction of Ni(II) occurred, the separation peak potential is 0.433 V, the ratio of ipa/ipc=1.32, indicating a quasi-reversible redox process. For Co(I)/Co(II), the redox couple cathodic peak appears at 0.240 in the absence of CT-DNA.

Table 1 Redox potential profiles for the interaction of DNA with synthesized complexes

Complexes	Redox couple	[a]$E_{1/2}$ (V)		[b]ΔEp (V)		I_{pa}/I_{pc}
		Free	Bound	Free	Bound	
1	Cu(II) → Cu(I)	−0.215	−0.228	0.426	0.451	1.38
	Cu(I) → Cu(0)	-0.343	-0.349	0.562	0.568	1.12
2	Co(II) → Co(I)	0.236	0.261	0.240	0.248	1.16
3	Ni(II) → Ni(I)	-0.208	-0.222	0.433	0.457	1.32
4	Zn(II) → Zn(0)	0.167	0.184	0.513	0.535	0.92

The ratio of i_{pc}/i_{pa} is approximately unity. This indicates that the reaction of the complex on the glassy carbon electrode surface is quasi-reversible redox process. The incremental addition of CT-DNA to the complex causes a positive shift in formal potential ($E_{1/2}$) indicating that [CoL_2] has bonded favorably with DNA via intercalation. Finally Zn(II) complex exhibits quasi-reversible transfer process with redox couple [Zn(II)→Zn(0)], the ratio of i_{pa}/i_{pc} is 0.92 V. This also indicates the quasi-reversible redox process of the metal complex. The incremental addition of CT-DNA to the complex also causes a positive shift in formal potential ($E_{1/2}$) indicating that [ZnL_2] stabilizes the duplex (GC pairs) by intercalation. From these above data, it is understood that all the synthesized complexes interact with DNA through intercalating way.

Data from cyclic voltammetric measurements: [a]$E_{1/2}$ = Ep_a / Ep_c/2; [a]$E_{1/2}$ is calculated as the average of anodic (E_{Pa}) and cathodic (Ep_c) peak potentials; [b]$\Delta Ep = Ep_a - Ep_c$.

3.8. Antimicrobial evaluation of ligand and its metal(II) complexes

Antimicrobial drugs are designed to inhibit/kill the infecting organisms and to have no minimal effect on the recipient. The results of the antimicrobial activity have been compared with the conventional bactericide Kanamycin and the fungicide Fluconazole used as the standards. The results achieved from these studies have been enlisted in Tables 2 and 3. The data of the antibacterial and anti-fungal activity indicated that the metal chelates are more active than the ligand. However, the increased biocidal properties after complexation can be very well explained by chelation theory [67]. The mechanism of the toxicity of the complexes with the ligands may be ascribed to the increase of the lipophilic nature of the complexes arising from chelation. Due to the complexity of biological system, it is rather difficult to stipulate the exact mechanism for such activities. The susceptibilities of all strains of bacteria and a fungus to the ligand and its corresponding mononuclear metal complexes were evaluated by measuring the minimum inhibitory concentration at which no growth was observed was taken as the MIC values. Comparison of MIC values (in lg/mL) of ligand, metal (II) complexes and standard drugs against different bacteria and fungi were presented in Tables 2 and 3. The results indicated that, these compounds were active in inhibiting the growth of tested organisms starting from 50 lg/mL concentration. Complex **1** appeared to have broad spectrum as it exhibits mild to moderate activity towards most of the strains. This study suggests that these complexes can further be explored as specific antimicrobial drugs due to their polite activity and less toxicity of metal ion.

Table 2 Minimum inhibitory concentration of the synthesized compounds against the growth of bacteria (μM)

Compounds	Minimum inhibitory concentration (MIC) (× 10^4 μM)				
	S. aureus	***B. subtilis***	***E. coli***	***K. pneumoniae***	***S. typhi***
L	20.1	20.9	21.2	21.7	22.1
1	9.2	9.5	9.6	9.9	10.3
2	9.4	9.7	9.8	10.2	10.6
3	9.5	9.9	10.4	10.8	11.0
4	9.7	10.1	10.5	11.1	11.4
[a]Kanamycin	1.6	2.8	1.4	2.3	2.6

[a] Kanamycin is used as the standard

Table 3 Minimum inhibitory concentration of the synthesized compounds against the growth of fungi (μM)

Compounds	**Minimum inhibitory concentration (MIC) (× 10^4 μM)**				
	A. niger	***F. solani***	***C. lunata***	***R. bataticola***	***C. albicans***
L	19.5	19.9	20.0	20.7	21.2
1	8.9	9.3	9.5	9.6	9.9
2	9.1	9.4	9.7	9.9	10.3
3	9.5	9.8	10.1	10.4	10.7
4	9.7	10.0	10.5	10.9	11.2
[a]Fluconazole	1.4	1.7	1.2	1.5	1.8

[a]Fluconazole is used as the standard

CONCLUSION

The present study revealed that, Schiff base of 8-aminoquinolone ring system can be used for improving the chemical status of the existing structures which have shown some anticancer activity.

REFERENCES

[1] www.who.com.
[2] L. Dobrek, P. Szczesniak, P. Thor, D. Orszulak-Michalak, Geriatria **2** (2008) 37–46.
[3] http://www.who.int/en/.
[4] O. Atakol, R. Bõca, I. Ercan, F. Ercan, H. Fuess, W. Haase, R. Herchel, Magnetic properties of trinuclear Ni–M–Ni complexes, M = Mn, Co and Ni, *Chem. Phys. Lett*. **423** (2006) 192-196.
[5] W. Liu, Y. Zou, C. Ni, Y. Li, Q. Meng, Synthesis, structural characterization and magnetic properties of new tripeptide Schiff base heterotrinuclear Cu(II)–M(II)–Cu(II) (M=Ni and Mn) complexes, *J. Mol. Struct*. **751** (2005) 1-6.
[6] R. Tao, C. Mei, S. Zang, Q. Wang, J. Niu, D. Liao, Synthesis, characterization, crystal structures and magnetic properties of dissymmetrical double Schiff base heterotrinuclear complexes: $[CuL(H_2O)CoCuL] \cdot H_2O \cdot CH_3OH$ and $[(CuL)_2Ni]\ 2H_2O$, *Inorg. Chim. Acta* **357** (2004) 1985-1990.
[7] N. Dharmaraj, P. Viswanathamurthi, K.Natarajan, Ruthenium(II) complexes containing bidentate Schiff bases and their antifungal activity, *Transit. Met. Chem*. **26** (2001) 105-109.
[8] S. Oz, R. Kurtaran, C. Arici, U. Ergun, F. N. D. Kaya, K. C. Emregul, O. Atakol, D. Ulku, Two non-linear azide containing heteronuclear complexes: crystal structure and thermal decomposition, *J. Therm. Anal. Calorim*. **99** (2010) 363-368.
[9] Y. Shibuya, K. Nabari, M. Kondo, S. Yasue, K. Maeda, F. Uchida, H. Kawaguchi, The copper(II) complex with two didentate Schiff base ligands. The unique rearrangment

that proceeds under alcohol vapor in the solid state to construct noninclusion structure, *Chem. Lett*. **37** (2008) 78-79.

[10] B. J. Gangani, P. H. Parsania, Microwave-irradiated and classical syntheses of symmetric double Schiff bases of 1,1′-bis(4-aminophenyl)cyclohexane and their physicochemical characterization, *Spectrosc. Lett*. **40** (2007) 97–112.

[11] B. S. Kumari, G. Rijulal, K. Mohanan, Microwave assisted synthesis, spectroscopic, thermal and biological studies of some lanthanide(III) chloride complexes with a heterocyclic schiff base, *Synth. React. Inorg. Metal-Org. nano-Met. Chem*. **39** (2009) 24–30.

[12] M. Thankamony, K. Mohanan, Synthesis, spectral studies, thermal decomposition kinetics, reactivity and antibacterial activity of some lanthanide(III) nitrate complexes of 2-(N-indole-2-one) amino-3-carboxyethyl-4,5,6,7-tetrahydrobenzo[b]thiophene, *Indian J. Chem. A*, **46** (2007) 247–251.

[13] N. Raman, J. D. Raja, A. Sakthivel, Synthesis, spectral characterization of Schiff base transition metal complexes: DNA cleavage and antimicrobial activity studies, *J. Chem. Sci*. **119** (2007) 303–310.

[14] B. Halli, V. B. Patil, Synthesis, spectral characterization and DNA cleavage studies of Co(II), Ni(II), Cu(II), Zn(II), Cd(II) and Hg(II) complexes with benzofuran-2-carbohydrazide schiff bases, *Indian J. Chem. A*, **50** (2011) 664–669.

[15] K. Shivakumar, M. B. Halli, Synthesis, characterization and antimicrobial studies on metal complexes with a naphthofuran thiosemicarbazide derivatives, *J. Coord. Chem*. **59** (2006) 1847–1856.

[16] P. R. Reddy, A. Shilpa, 2-Hydroxynaphthalene-1-carbaldehyde- and 2-(aminomethyl)pyridine-based Schiff base CuII complexes for DNA binding and cleavage, *Chem. Biodivers*. **9** (2012) 2262-2281.

[17] T.D. Nguyen, T.T. Duong, T.P. Quynh Le, V.M. Chau, M.H. Le, D.K. Dang, J.J. Lee, M. Lise B. Kondracki, Inhibitory effects on nuclear factor κB of the Vietnamese fresh water cyanobacteria, *Med. Chem. Res*. **20** (2011) 790-793.

[18] A. Castonguay, C. Doucet, M. Juhas, D. Maysinger, New Ruthenium(II)–Letrozole Complexes as Anticancer Therapeutics, *J. Med. Chem.* **55** (2012) 8799–8806.

[19] O. Pinato, C. Musetti, N.P. Farrell, C. Sissi, Platinum-based drugs and proteins: Reactivity and relevance to DNA adduct formation, *J. Inorg. Biochem*. **122** (2013) 27-37.

[20] C.R. Cauadine, H.R. Drew, B.F. Luisi, A.A. Travers, Understanding DNA: The molecule and How it works, 3rd Ed., Elsevier Academic, San Diego, 2004.

[21] M.A. Fuertes, C. Alonso, J.M. Pérez, Biochemical modulation of cisplatin mechanisms of action: enhancement of antitumor activity and circumvention of drug resistance, *Chem. Rev.*, **103(3)** (2003) 645–662.

[22] N.G. Faux, C.W. Ritchie, A. Gunn, A. Rembach, A. Tsatsanis, J. Bedo, J. Harrison, L. Lannfelt, K. Blennow, H. Zetterberg, M. Ingelsson, C.L. Masters, R.E. Tanzi, J.L. Cummings, C.M. Herd, A.I. Bush, PBT2 rapidly improves cognition in Alzheimer's disease: additional phase II analyses, *J. Alzheimers Dis*. **20** (2010) 509-516.

[23] S.K. Prashant, A.K. Dutta, *Curr. Bioact. Compd*. **4** (2008) 57.

[24] A.I. Bush, R.E. Tanzi, Therapeutics for Alzheimer's disease based on the metal hypothesis, *Neurotherapeutics* **5** (2008) 421-432.

[25] K.J. Barnham, E. Gautier, L. Colette, G.B. Kong, G. Krippner, 8-hydroxy quinoline derivatives, WO 2004/007461, 2004.

[26] H.R. Dholariya, K.S. Patel, J.C. Patel, A.K. Patel, K.D. Patel, Thermal, kinetic, spectroscopic studies and anti-microbial, anti-tuberculosis, anti-oxidant properties of

clioquinol and benzo-coumarin derivatives mixed complexes with copper ion, *Med. Chem. Res*. **22** (2013) 5848-5860.

[27] B. Choi, J. Young, G. Bong, J.H. Kim, J.-N. Seo, G. Wu, M. Sohn, T.N. Chung, S.W. Suh, Copper/zinc chelation by clioquinol reduces spinal cord white matter damage and behavioral deficits in a murine MOG-induced multiple sclerosis model, *Neurobiol. Dis*. **54** (2013) 382-391.

[28] A.D. Schimmer, Y. Jitkova, M. Gronda, Z. Wang, J. Brandwein, C. Chen, V. Gupta, A. Schuh, K. Yee, J. Chen, S. Ackloo, T. Booth, S. Keays, M.D. Minden, A Phase I Study of the metal ionophore clioquinol in patients with advanced hematologic malignancies, *Clin. Lymphoma Myeloma Leuk*. **12** (2012) 330-336.

[29] C.M. Darby, C.F. Nathan, Killing of non-replicating *Mycobacterium tuberculosis* by 8-hydroxyquinoline, *J. Antimicrob. Chemother*. **65** (2010) 1424-1427.

[30] H. Jiang, J.E. Taggart, X. Zhang, D.M. Benbrook, S.E. Lind, W.-Q. Ding, Nitroxoline (8-hydroxy-5-nitroquinoline) is more a potent anti-cancer agent than clioquinol (5-chloro-7-iodo-8-quinoline), *Cancer Lett*. **312** (2011) 11-17.

[31] K.G. Daniel, D. Chen, S. Orlu, Q.C. Cui, F.R. Miller, Q.P. Dou, Clioquinol and pyrrolidine dithiocarbamate complex with copper to form proteasome inhibitors and apoptosis inducers in human breast cancer cells, *Breast Cancer Res*. **7** (2005) R897-R908.

[32] X. Mao, X. Li, R. Sprangers, X. Wang, A. Venugopal, T. Wood, Y. Zhang, D.A. Kuntz, E. Coe, S. Trudel, D. Rose, R.A. Batey, L.E. Kay, A.D. Schimmer, Clioquinol inhibits the proteasome and displays preclinical activity in leukemia and myeloma, *Leukemia* **23** (2009) 585-590.

[33] D. Chen, Q.C. Cui, H. Yang, R.A. Barrea, F.H. Sarkar, S. Sheng, B. Yan, G.P. Reddy, Q.P. Dou, Clioquinol, a therapeutic agent for Alzheimer's disease, has proteasome-inhibitory, androgen receptor-suppressing, apoptosis-inducing, and antitumor activities in human prostate cancer cells and xenografts, *Cancer Res*. **67** (2007) 1636-1644.

[34] S. Zhai, L. Yang, Q.C. Cui, Y. Sun, Q.P. Dou, B. Yan, Tumor cellular proteasome inhibition and growth suppression by 8-hydroxyquinoline and clioquinol requires their capabilities to bind copper and transport copper into cells, *J. Biol. Inorg. Chem*. **15** (2010) 259-269.

[35] H. Yu, Y. Zhou, S.E. Lind, W.Q. Ding, Clioquinol targets zinc to lysosomes in human cancer cells, *Biochem. J*. **417** (2009) 133-139.

[36] W.Q. Ding, B. Liu, J.L. Vaught, H. Yamauchi, S.E. Lind, Anticancer activity of the antibiotic clioquinol, *Cancer Res*. **65** (2005) 3389-3395.

[37] H. Yu, J.R. Lou, W.Q. Ding, Clioquinol independently targets NF-kappaB and lysosome pathways in human cancer cells, *Anticancer Res*. **30** (2010) 2087-2092.

[38] T. Du, G. Filiz, A. Caragounis, P.J. Crouch, A.R. White, Clioquinol promotes cancer cell toxicity through tumor necrosis factor α release from macrophages, *J. Pharmacol. Exp. Ther*. **324** (2008) 360-367.

[39] N. Bharti, S. Sharma, F. Naqvi, A. Azam, New palladium(II) complexes of 5-nitrothiophene-2-carboxaldehyde thiosemicarbazones: synthesis, spectral studies and *in vitro* anti-amoebic activity, *Bioorg. Med. Chem*. **11** (2003) 2923–2929.

[40] A. Soliman, Synthesis and properties of new substituted 1,2,4-triazoles: potential antitumor agents, *J. Therm. Anal. Calcul*. **63** (2001) 221.

[41] F. Petrovic, D. M. Petrovic, V. M. Leovac, M. Budimir, Ruthenium(II) complexes containing bidentate Schiff bases and their antifungal activity, *J. Therm. Anal. Calcul.* **58** (1999) 589.

[42] Ivanovic, K. Andjelkovic, V. M. Leovac, L. J. Klisarov, M. Lazavevic, and D. Minic, Molecular design of mononuclear complexes of acyclic Schiff-base ligands, *J. Coord. Chem*. **46** (1996) 1741.
[43] D.D. Perrin, W.L.F. Armarego, D.R. Perrin, Purification of laboratory chemicals, Oxford, U.K, 1980.
[44] G. Kumaravel, N. Raman, A treatise on benzimidazole based Schiff base metal(II) complexes accentuating their biological efficacy: Spectroscopic evaluation of DNA interactions, DNA cleavage and antimicrobial screening, *Mater. Sci. Eng. C* **70** (2017) 184-194.
[45] G. Kumaravel, P. Ponya Utthra, N. Raman, DNA fastening and scission actions of Cu(II), Co(II), Ni(II) and Zn(II) complexes: synthesis, spectral characterization and cytotoxic study, *Appl. Organomet. Chem*. (2017) doi: 10.1002/aoc.4010.
[46] W.G. Geary, The use of conductivity measurements in organic solvents for the characterisation of coordination compounds, *Coord. Chem. Rev*. **7** (1971) 81–122.
[47] A. Manimaran, C. Jayabalakrishnan, Synthesis, characterization, redox, catalytic, and antibacterial activities of binuclear ruthenium(III) Schiff base complexes containing triphenylphosphine as co-ligand, *Synth. React. Inorg. Met.-Org. Nano-Metal Chem*. **40** (2010) 116–128
[48] N. Shahabadi, S. Kashanian, F. Darabi, DNA binding and DNA cleavage studies of a water soluble cobalt(II) complex containing dinitrogen Schiff base ligand: The effect of metal on the mode of binding, *Eur. J. Med. Chem*. **45** (2010) 4239–4245.
[49] M. Türner, K. Hüseyin, S. Serin, S. Patat, Synthesis and characterization of some cobalt(II), nickel(II) and zinc (II) complexes with Schiff bases derived from the reaction of 4-hydroxysalicylaldehyde and *o*-vanillin with 3,5-di(tert-butyl)-4-hydroxyaniline, *Synth. React. Inorg. Met.-Org. Nano-Metal Chem*. **27** (1997) 59–68.
[50] K. Nakamato, Infrared and Raman spectra of inorganic and coordination compounds, Wiley Interscience, New York, 1971.
[51] L. Antolini, L. Menabue, G.C. Pellacani, M. Saladin, L.P. Batuglia, A.B. Corradi, G. Marcotrigian, Notes. magnetic and spectroscopic properties of dimeric copper(II) complexes of N-benzyloxycarbonyl-substituted amino acid anions, *J. Chem. Soc. Dalton Trans*. **10** (1984) 2325-2326.
[52] S. Budagumpi, M.P. Sathisha, N. V. Kulkarni, G.S. Kurdekar, V.K. Revankar, Transition metal complexes of pyrazole head 24-membered polyazamacrocyclic bimetal cores: synthesis, characterization, electrochemistry and spectral study, *J. Incl. Phenom. Macrocycl. Chem*. **66** (2010) 327-333.
[53] A.B.P. Lever, Inorganic electronic spectroscopy, 2nd Edn., Elsevier, Amsterdam, 1984.
[54] B.N. Figgis, J. Lewis, Modern coordination chemistry: principles and methods, in: J. Lewis, R.G. Wilkins (Eds.), Interscience, New York, 1960.
[55] N. Raman, S. Ravichandran, C. Thangaraja, Copper(II), cobalt(II), nickel(II) and zinc(II) complexes of Schiff base derived from benzil-2,4-dinitrophenylhydrazone with aniline, *J. Chem. Sci*. **116** (2004) 215-219.
[56] G. Kumaravel, P. Ponya Utthra, N. Raman, Exploiting the biological efficacy of benzimidazole based Schiff base complexes with L-histidine as a co-ligand: Combined molecular docking, DNA interaction, antimicrobial and cytotoxic studies, *Bioorg. Chem*. **77** (2018) 269–279.
[57] S. Sobha, R. Mahalakshmi, N. Raman, Studies on DNA binding behaviour of biologically active transition metal complexes of new tetradentate N_2O_2 donor Schiff bases: Inhibitory activity against bacteria, *Spectrochim. Acta A* **92** (2012) 175–183.

[58] M. Patil, R. Hunoor, K. Gudasi, Transition metal complexes of a new hexadentate macroacyclic N_2O_4-donor Schiff base: Inhibitory activity against bacteria and fungi, *Eur. J. Med. Chem*. **45** (2010) 2981–2986.
[59] S. Tabassum, A. Asim, F. Arjmand, M. Afzal, V. Bagchi, Synthesis and characterization of copper(II) and zinc(II)-based potential chemotherapeutic compounds: Their biological evaluation *viz*. DNA binding profile, cleavage and antimicrobial activity, *Eur. J. Med. Chem*. **58** (2012) 308–316.
[60] D.S. Raja, N.S.P. Bhuvanesh, K. Natarajan, Biological evaluation of a novel water soluble sulphur bridged binuclear copper(II) thiosemicarbazone complex, *Eur. J. Med. Chem*. **46** (2011) 4584–4594.
[61] N. Pravin, G. Kumaravel, R. Senthilkumar, N. Raman, Water-soluble Schiff base Cu(II) and Zn(II) complexes: Synthesis, DNA targeting ability and chemotherapeutic potential of Cu(II) complex for hepatocellular carcinoma–*in vitro* and *in vivo* approach, *Appl. Organometal. Chem*. (2016) DOI 10.1002/aoc.3739.
[62] Y. J. Liu, W.J. Mei, J.Z. Lu, H.J. Zhao, L.X. He, F.H. Wu, Ruthenium(II) complexes of 2-(2′-pyridyl)naphthoimidazole: synthesis, characterization and DNA-binding studies, *J. Coord. Chem*. **61** (2008) 3213–3224.
[63] A.A. Ibrahim, A.M. Adel, Z.H. Abd El-Wahab, M.T. Al-Shemy, Utilization of carboxymethyl cellulose based on bean hulls as chelating agent. Synthesis, characterization and biological activity, *Carbohydr. Polym*. **83** (2011) 94-115.
[64] F. Boussicault, M. Robert, Electron transfer in DNA and in DNA-related biological processes. electrochemical insights, *Chem. Rev*. **108** (2008) 2622-2645.
[65] (a) R. Indumathy, S. Radhika, M. Kanthimathi, T. Weyhermuller, B. Unni Nair, Cobalt complexes of terpyridine ligand: Crystal structure and photocleavage of DNA, *J. Inorg. Biochem*. **101** (2007) 434–443; (b) M.H. Habibi, E. Shojaee, M. Ranjbar, H.R. Memarian, A. Kanayama, T. Suzuki, Computational and spectroscopic studies of a new Schiff base 3-hydroxy-4-methoxybenzylidene(2-hydroxyphenyl)amine and molecular structure of its corresponding zwitterionic form, *Spectrochim. Acta A* **105** (2013) 563–568.
[66] (a) P. Ponya Utthra, G. Kumaravel, R. Senthilkumar, N. Raman, Heteroleptic Schiff base complexes containing terpyridine as chemical nucleases and their biological potential: A study of DNA binding and cleaving, antimicrobial and cytotoxic tendencies, *Appl. Organometal. Chem*. (2016) doi 10.1002/aoc.3629; (b) Y. Ni, D. Lin, S. Kokat, *Anal. Biochem*. **352** (2006) 23.
[67] R.V. Singh, A. Chaudhary, Biologically relevant tetraazamacrocyclic complexes of manganese: synthetic, spectral, antimicrobial, antifertility and antiinflammatory approach, *J. Inorg. Biochem*. **98** (2004) 1712–1721.